J. Fluid Mech. (1967), *vol.* 28, *part* 2, *pp.* 371–384
Printed in Great Britain

Hartmann flow in an annular channel

By L. TODD
Department of Mathematics, Massachusetts Institute of Technology†

(Received 5 April 1966 and in revised form 18 October 1966)

Flow at high Hartmann number along the annular channel between two non-conducting cylinders of circular cross-section is examined. The core is divided and wakes appear at the boundaries of the various regions. In §§ 1–4 the case in which the cylinders are concentric is studied. In § 5 the cylinders are eccentric, and it is shown that in this case there is a net flow of current around the annulus.

1. Introduction

The problem of pressure-driven flow of conducting fluid through an insulating pipe of circular cross-section in the presence of a transverse magnetic field has been analysed by Shercliff (1956, 1962) and Gold (1962). The exact solution may be obtained in the form of an infinite series, from which useful information may be extracted numerically. At high Hartmann number, however, a boundary layer analysis is more illuminating, and indicates that there are essentially three régimes in the flow: a core in which the velocity is uniform, a Hartmann layer on the boundary, and 'obscure regions' in the neighbourhood of the points on the boundary where the applied field is tangential to the pipe.

In this paper Shercliff's high Hartmann number analysis is extended to the case of pressure-driven flow through the annular channel between two insulating cylinders of circular cross-section. The equations that describe the flow are the linear equations first derived by Shercliff (1953); only the boundary conditions are changed. It has been observed by Uflyand (1961) that, when the cylinders are concentric, the exact solution may again be obtained in the form of an infinite series. For large Hartmann number, however, the series converges extremely slowly, and its usefulness is questionable. Hence it seems worthwhile to exploit boundary-layer techniques in order to obtain the main properties of the solution in this limit.

Several interesting features emerge from the analysis; in particular, the core flow is divided (see figure 8) by transition regions (or, loosely, 'wakes') in the neighbourhood of the planes parallel to the applied field $\mathbf{B}_0$ and tangential to the inner cylinder. These wakes are of a type first analysed by Hasimoto (1960) in a treatment of the flow generated by the motion of a cylinder parallel to its generators in a fluid of infinite extent. (The work of the present paper can easily be extended to allow for steady motion of the inner cylinder parallel to its axis.)

† Present address: Department of Mathematics, Strathclyde University, Glasgow C. 1.

2. The governing equations and boundary conditions

The governing equations for unidirectional flow in a transverse applied magnetic field (Shercliff 1953) are

$$\lambda\nabla^2 B_z + B_0\frac{\partial V_z}{\partial x} = 0, \tag{1}$$

$$\rho\nu\nabla^2 V_z + \frac{B_0}{\mu}\frac{\partial B_z}{\partial x} = -P, \tag{2}$$

$$\frac{\partial}{\partial x}, \frac{\partial}{\partial y}\left(p + \frac{B_z^2}{2\mu}\right) = 0. \tag{3}$$

The notation is standard; $B = (B_0, 0, B_z)$, where B_0 is the (constant) applied magnetic field, $-P = \partial p/\partial z$ = constant, and λ and ν are the magnetic and shear diffusivities respectively. The third equation indicates the absence of forces tending to move the fluid across the pipe. $\hat{\mathbf{z}}B_z$ is the vector potential for the current density vector. In our geometry this means that B_z is the stream function for current, i.e. current flows along the lines B_z = constant.

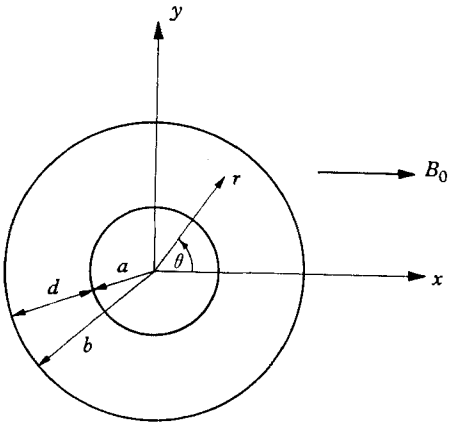

FIGURE 1. The rotation for concentric cylinders.

Consider the case of pressure-driven flow through the annular channel between the concentric cylinders $r = a, b (b > a)$.

Let

$$q = P\{(\rho\nu\sigma)^{\frac{1}{2}}B_0\}^{-1}, \quad s = \mu^{-1}(\sigma\rho\nu)^{-\frac{1}{2}}, \tag{4), (5}$$

$$m = V_z + (qx + sB_z), \quad n = V_z - (qx + sB_z), \tag{6), (7}$$

and $2\beta = B_0(\sigma/\rho\nu)^{\frac{1}{2}}$ (the Hartmann wave number). Equations (1) and (2) then become

$$\nabla^2 m + 2\beta\frac{\partial m}{\partial x} = 0, \quad \nabla^2 n - 2\beta\frac{\partial n}{\partial x} = 0. \tag{8), (9}$$

The velocity V_z must vanish at the boundaries. B_z may be assumed to vanish at $r = b$. At $r = a$ the radial current must vanish and this requires

$$B_z = \text{constant} = C \text{ (say)}.$$

The value of B_z within the inner cylinder is also C, since there $\nabla^2 B_z = 0$. Moreover, since curl $\mathbf{E} = -(\partial \mathbf{B}/\partial t) = 0$ under steady conditions, it follows that

$$\int_0^{2\pi} E_\theta(a, \theta)\, d\theta = 0, \quad \text{and as} \quad j_\theta = (\sigma E_\theta) \quad \text{at} \quad r = a+,$$

this boundary condition may be written (Hasimoto 1960)

$$\int_0^{2\pi} \left(\frac{\partial B_z}{\partial r}\right)_{r=a+} d\theta = 0. \tag{10}$$

3. The value of B_z at the inner cylinder

It follows from $\mu \mathbf{j} = \text{curl}\, \mathbf{B}$ that $(B_z)_{r=a} = C = \mu I$, where I is the net amount of current flowing around the annulus per unit length. It will now be shown that the symmetry about the y-axis implies that $I = 0$. This is done by separating the linear problem (1), (2) into two parts. The solutions will be added together and then the boundary condition (10) will be applied.

(i) First, suppose that equations (1) and (2) are solved subject to the boundary conditions $V_z = 0 = B_z$ on $r = a$ and $r = b$.

The solution obviously has the property $B_z(x) = -B_z(-x)$ and it follows that equation (10) is satisfied.

(ii) Secondly, suppose that the equations

$$\lambda \nabla^2 B_z + B_0 \frac{\partial V_z}{\partial x} = 0, \tag{11}$$

$$\rho \nu \nabla^2 V_z + \frac{B_0}{\mu} \frac{\partial B_z}{\partial x} = 0, \tag{12}$$

are solved, subject to the boundary conditions

$$V_z = 0 \quad \text{at} \quad r = a, b; \quad B_z = 0 \quad \text{at} \quad r = b;$$
$$B_z = C \text{ (constant)} \quad \text{at} \quad r = a.$$

Since the condition (10) is satisfied by the solution of problem (i), the solution of (ii) must also satisfy (10), in order that the sum of the two solutions is the solution to the problem set out in § 2. From equations (11) and (12),

$$\iint_S \left\{\lambda B_z \nabla^2 B_z + \frac{\nu}{\lambda} V_z \nabla^2 V_z + B_0 \frac{\partial}{\partial x}(V_z B_z)\right\} dS = 0,$$

where S is the area of the annulus between $r = a$ and $r = b$. The third form in this integral is obviously zero; moreover

$$\iint_S V_z \nabla^2 V_z dS = -\iint_S (\nabla V_z)^2 dS,$$

since $V_z = 0$ at the boundaries, and

$$\iint_S (B_z \nabla^2 B_z) dS = -\iint_S (\nabla B_z)^2 dS - aC \int_{\theta=0}^{2\pi} \left(\frac{\partial B_z}{\partial r}\right)_{a+} d\theta = -\iint_S (\nabla B_z)^2 dS,$$

using (10). It follows that $\nabla B_z \equiv 0$ and $\nabla V_z = 0$. Since $B_z \equiv 0$ at $r = b$, it follows that $C = 0$, and hence that $I = 0$.

This result depends only on symmetry about the y-axis. Thus, it is true for any number of cylinders of any cross-section, provided that the outer one and all the

inner ones have this symmetry. When this condition is not met, the determination of the value of B_z at each of the inner cylinders is more complicated. With very little modification, the analysis for problem (*b*) will show that the solution for such Hartmann flows is unique.

4. The flow at large Hartmann number

The flow in the case of concentric circular cylinders depends on the Hartmann number

$$M = B_0(\sigma/\rho\nu)^{\frac{1}{2}}a \tag{13}$$

and on the geometrical parameter d/a ($d = b-a$). We investigate the asymptotic nature of the flow as $M\to\infty$ under the assumption that $d/a = O(1)$. [If $d/a = O(M^{-1})$, for example, then the results obtained below are invalid.]†

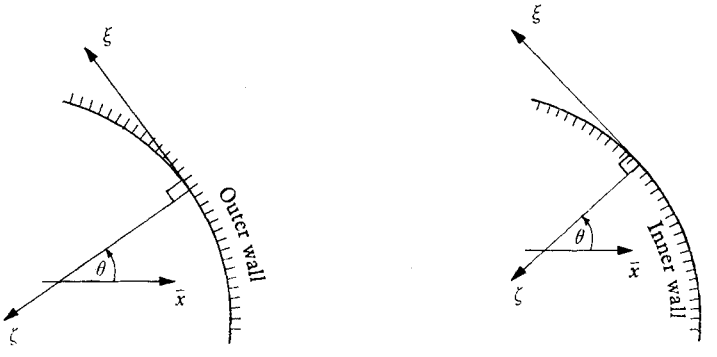

FIGURE 2. The boundary-layer co-ordinates.

We shall seek core solutions, together with thin Hartmann boundary layers on the walls. This approach was used by Shercliff (1956) for flow through a circular cylinder. It is valid provided $M \geqslant 1$. However, we shall find wakes near $|y| = a$. In order to discuss these, it is necessary that

$$M^{\frac{1}{2}} \gg 1. \tag{14}$$

(i) *Hartmann boundary layers at the walls*

The boundary-layer co-ordinates (ξ, ζ) are shown in figure 2. ζ measures distance along the inward radius. (ξ, ζ, z) form a right-handed set of Cartesian co-ordinates. Equation (8) now becomes

$$a\left(\frac{\partial^2 m}{\partial\zeta^2}+\frac{\partial^2 m}{\partial\xi^2}\right) - M\cos\theta\frac{\partial m}{\partial\zeta} - M\sin\theta\frac{\partial m}{\partial\xi} = 0. \tag{15}$$

Following Shercliff (1956) we seek boundary-layer solutions, near the walls, in which $\partial/\partial\zeta \gg \partial/\partial\xi$. Thus, provided we are not 'too near' $|\theta| = (\frac{1}{2}\pi)$, equation (15) can be approximated by

$$a\frac{\partial^2 m}{\partial\zeta^2} - M\cos\theta\frac{\partial m}{\partial\zeta} = 0, \tag{16}$$

with solution

$$m = m_{\text{core}} + C_1\exp\{(\cos\theta)M\zeta a^{-1}\}, \tag{17}$$

† C. J. Apelt (private communication) has analysed the problem numerically in the range $0 \leqslant M \lesssim 25$ for both concentric and eccentric cylinders and his results are consistent with the analysis of this paper for $M \gtrsim 5$.

where m_{core} and C_1 are possibly functions of ξ. It follows that m has boundary layers only on that portion of the outer wall for which $\cos\theta < 0$, $\zeta \geqslant 0$. On the right-hand part of the outer wall, m does not have a boundary layer and thus equation (16) does not apply there. Similarly, equations (16) and (17) only apply near that portion of the inner boundary where $\cos\theta > 0$ and $\zeta \leqslant 0$. These results are illustrated in figure 3(*a*). In the boundary-layer co-ordinates, equation (9) is

$$a\left(\frac{\partial^2 n}{\partial\zeta^2}+\frac{\partial^2 n}{\partial\xi^2}\right)+M\cos\theta\frac{\partial n}{\partial\zeta}+M\sin\theta\frac{\partial n}{\partial\xi}=0. \tag{18}$$

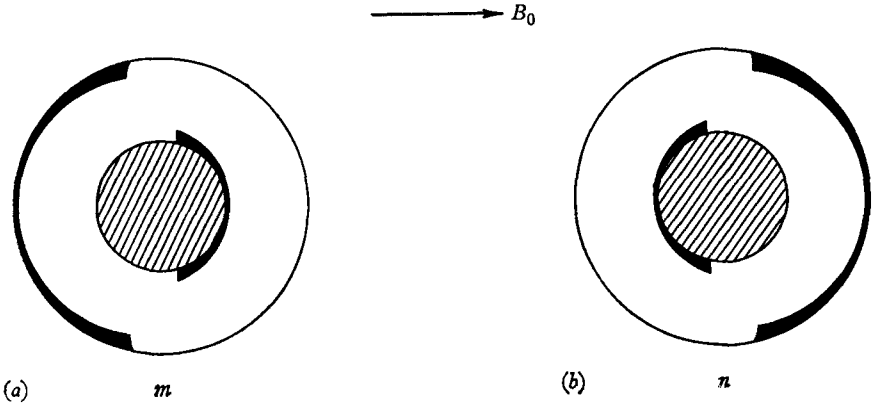

FIGURE 3. The boundary layers.

To the above approximation, equation (18) becomes

$$a\frac{\partial^2 n}{\partial\zeta^2}+M\cos\theta\frac{\partial n}{\partial\zeta}=0, \tag{19}$$

with solution
$$n = n_{\text{core}}+C_2\exp\{-(\cos\theta)M\zeta a^{-1}\}, \tag{20}$$

where n_{core} and C_2 may be functions of ξ. It follows that n has boundary layers as indicated in figure 3(*b*) and that equations (19) and (20) are valid only in these regions.

Let us now find out at what value of $|\theta|$ the theory breaks down. Now, since $\partial/\partial\xi = r^{-1}(\partial/\partial\theta)$, m_{core}, n_{core} and C_1, C_2 may all vary with θ. However, it will be shown at a later stage that, in every case of interest in this paper, the order† of magnitude of the ξ-derivative is given by treating the four latter quantities as constants. One of the neglected terms, $(M\sin\theta(\partial/\partial\xi))$, becomes of the same order as the two retained terms in (15) or (18), at values of $|\theta|$ near $\frac{1}{2}\pi$ for which

$$aM^2\cos^2\theta \sim Ma\,|\tan\theta|, \tag{21}$$

i.e.
$$|(\tfrac{1}{2}\pi)-|\theta|| \sim M^{-\frac{1}{3}}. \tag{22}$$

The width of the boundary layer at the edge of the region indicated by (22) is of order $rM^{-\frac{2}{3}}$ on the two cylinders $r = a, b$ (see figure 4).

† Hereafter we shall use the symbol $\sim$ to mean 'of the order of'.

(ii) *The core solutions*

Let us now examine conditions outside the boundary layers. The region $|y| > a$ may be described as the outer core. In the left inner core, $|y| < a$ and $x < O$, and in the right inner core, $|y| < a$ and $x > O$. The values of m and n in these regions are labelled by the suffices O, L and R, respectively.

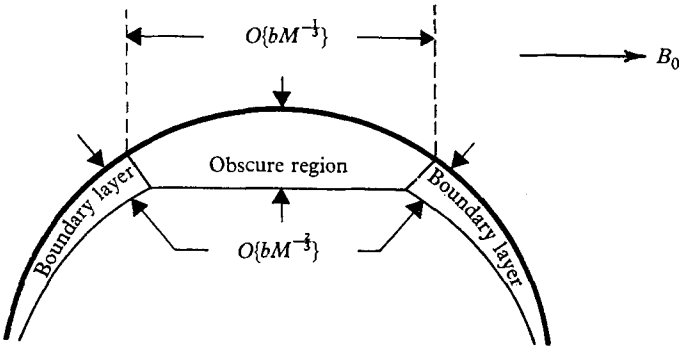

FIGURE 4. The obscure region on the outer cylinder near $\theta = +(\frac{1}{2}\pi)$.

On the right-hand side of the outer wall, $m = q(b^2-y^2)^{\frac{1}{2}}$ and there is no boundary layer. It is reasonable to assume that at points near to this boundary the length scale of variation in the y-direction, L_y, is determined by the value of m *at* the wall, i.e.

$$L_y \sim (b^2-y^2)y^{-1}. \tag{23}$$

Thus, provided we are not too near, $|y| = b$, $L_y \sim b$ (or greater). Now

$$a\left(\frac{\partial^2 m}{\partial y^2}+\frac{\partial^2 m}{\partial x^2}\right)+M\frac{\partial m}{\partial x}=0,$$

so that $L_x \sim bM$ (or greater), i.e., to highest order, there is no x-variation of m. This suggests that, for the outer core and right inner core, we seek an expansion of the form

$$m = q(b^2-y^2)^{\frac{1}{2}}+f_1(x,y)M^{-1}+f_2(x,y)M^{-2}+\ldots.$$

It can easily be shown that

$$m_R = m_0 = q(b^2-y^2)^{\frac{1}{2}}+qb^2aM^{-1}\{x(b^2-y^2)^{-\frac{1}{2}}-1\}(b^2-y^2)^{-1}+O(mM^{-2}). \tag{24}$$

Equation (24) is not valid for the left inner core, since L_y in this region is derived from the behaviour of m on the left-hand wall of the inner cylinder. On this boundary, $m = -q(a^2-y^2)^{\frac{1}{2}}$. Thus, except near $|y| = a$, $L_y \sim (a^2-y^2)y^{-1} \sim a$ (or greater), so that $L_x \sim aM$ (or greater). Consequently, we obtain the expansion

$$m_L = -q(a^2-y^2)^{\frac{1}{2}}-qa^3M^{-1}\{x(a^2-y^2)^{-\frac{1}{2}}+1\}(a^2-y^2)^{-1}+O(mM^{-2}), \tag{25}$$

for the left inner core.

Now, $m_0 \neq m_L$ at $|y| = a$. In fact to highest order $m_0-m_L = q(b^2-a^2)^{\frac{1}{2}} =$ constant, at $|y| = a$. It is therefore to be expected that there will be two 'wakes', one centred at $y = +a$ and one at $y = -a$. This is illustrated in figure 5(*a*). These wakes are discussed in §4(iv).

In a similar way we obtain an expansion for n, which is valid in the outer and left inner core,

$$n_L = n_0 = q(b^2-y^2)^{\frac{1}{2}} - qb^2aM^{-1}\{x(b^2-y^2)^{-\frac{1}{2}}+1\}(b^2-y^2)^{-1}+O(nM^{-2}). \quad (26)$$

In the right inner core, L_y is derived from the behaviour of n on the right-hand boundary of the inner cylinder. Consequently, we obtain

$$n_R = -q(a^2-y^2)^{\frac{1}{2}}+qa^3M^{-1}\{x(a^2-y^2)^{-\frac{1}{2}}-1\}(a^2-y^2)^{-1}+O(nM^{-2}). \quad (27)$$

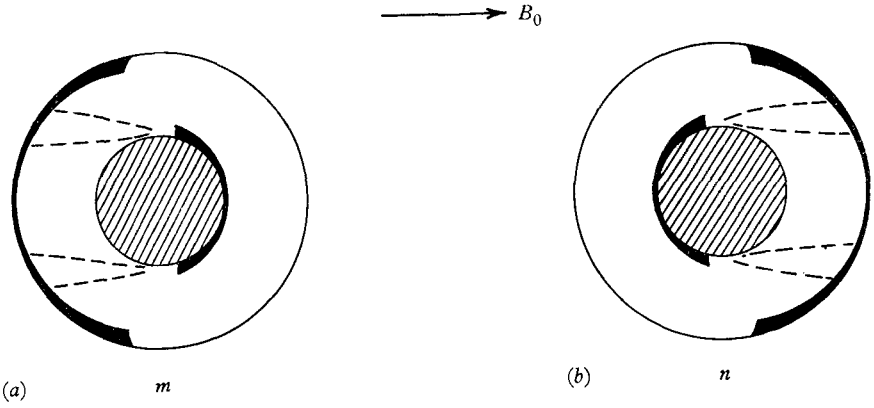

FIGURE 5. The transition regions, or 'wakes'.

We now determine where our core expansions will *not* be valid. The cases for m and n are quite similar. We will first consider the expansion for m in the outer and right inner core. The second term becomes of the same order of magnitude as the leading term where

$$(b-|y|) \sim bM^{-\frac{2}{3}}. \quad (28)$$

It can easily be checked that, at values of y satisfying (28), the length scale in the x-direction becomes of the same order as the local width of the duct. This is why the above expansion procedure breaks down. The expansion for n in the outer and left inner core breaks down at the same place. The first and second terms in the two remaining (inner) core expansions become of the same order of magnitude where

$$(a-|y|) \sim (a|x|/M)^{\frac{1}{2}}. \quad (29)$$

Again, this result is easy to understand. The length scale in the x-direction decreases to zero as $|y| \to a$. Thus the section of the flow to which the Taylor series expansions (about the inner wall) apply is bounded as set out in (29).

The values of V_z and B_z in each of the core regions are given below. V_z is even in x and y. B_z is odd in x and even in y.

Outer core

$$\left.\begin{aligned} V_z &= q\{(b^2-y^2)^{\frac{1}{2}} - aM^{-1}b^2(b^2-y^2)^{-1}\}+O\{(V_z)M^{-2}\}, \\ B_z &= -\mu PxB_0^{-1}+a\mu Pb^2x\{2B_0M(b^2-y^2)^{\frac{3}{2}}\}^{-1}+O\{(B_z)M^{-2}\}; \end{aligned}\right\} \quad (30)$$

Left inner core

$$\left.\begin{aligned} V_z &= 2^{-1}q\{(b^2-y^2)^{\frac{1}{2}}-(a^2-y^2)^{\frac{1}{2}}-D_+(b)-D_+(a)\}, \\ &\text{where} \\ D_\pm(r) &= ar^2M^{-1}\{x(r^2-y^2)^{-\frac{1}{2}}\pm 1\}(r^2-y^2)^{-1}, \\ B_z &= -\mu PxB_0^{-1}-\mu P2^{-1}B_0^{-1}\{(b^2-y^2)^{\frac{1}{2}}+(a^2-y^2)^{\frac{1}{2}}-D_+(b)+D_+(a)\}; \end{aligned}\right\} \quad (31)$$

Right inner core

$$\left.\begin{aligned} V_z &= 2^{-1}q\{(b^2-y^2)^{\frac{1}{2}}-(a^2-y^2)^{\frac{1}{2}}+D_-(b)+D_-(a)\}, \\ B_z &= -\mu PxB_0^{-1}+\mu P2^{-1}B_0^{-1}\{(b^2-y^2)^{\frac{1}{2}}+(a^2-y^2)^{\frac{1}{2}}+D_-(b)-D_-(a)\}. \end{aligned}\right\} \quad (32)$$

(iii) *The obscure regions, near $\theta = \pm\frac{1}{2}\pi$, on the outer cylinder*

The results of the last section and the fact that $m = n = 0$ on the walls, give the values of $m_{\text{core}}, n_{\text{core}}, C_1$ and C_2. The assumption made in § 4 (i) can then be verified. Thus the boundary-layer theory breaks down at precisely the same place as the

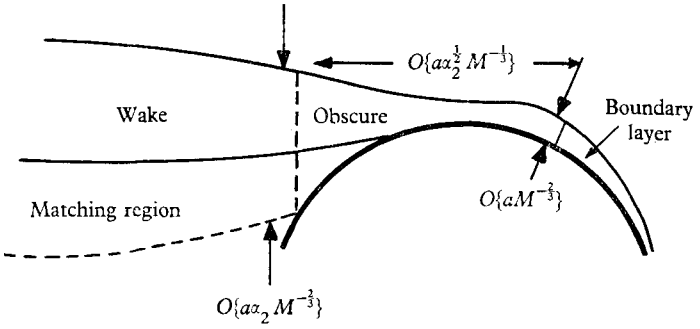

FIGURE 6. The obscure region, for m, on the inner cylinder near $\theta = \frac{1}{2}\pi$.

outer core expansion. This leaves an obscure region† of extent $bM^{-\frac{1}{3}}$, and the height $bM^{-\frac{2}{3}}$, as shown in figure 4. Though m and n have boundary layers on only one side of the outer wall, the physical quantities V_z and B_z have boundary layers on both sides. The value of V_z at the edge of the obscure region can be estimated from equation (30), it is $O(qbM^{-\frac{1}{3}})$. Thus Q_s, the contribution to the flow rate from the obscure region, is of order

$$Q_s \sim qb^3M^{-\frac{4}{3}}. \quad (33)$$

(iv) *The wakes and the obscure regions on the inner cylinders*

The 'wakes' might equally be called shear layers or transition layers. We will restrict the discussion to the behaviour of m. The analogous results for n will be stated at the end of the section. As was noted in the previous section, the boundary layer breaks down as given in § 4 (i). This is illustrated in figure 6.

† The results concerning the extent and thickness of the obscure region were first obtained by T. Waechter (private communication) in the closely related problem of the steady motion of a cylinder parallel to its axis (Hasimoto 1960) by rigorous asymptotic expansion of the exact solution.

Within the wakes we expect that $\partial/\partial y \gg \partial/\partial x$. Thus equation (8) becomes, to highest order,

$$a\frac{\partial^2 m}{\partial y^2} + M\frac{\partial m}{\partial x} = 0. \tag{34}$$

The appropriate similarity solution (cf. Hasimoto 1960) is

$$m = \tfrac{1}{2}q(b^2-a^2)^{\frac{1}{2}}\{1+\operatorname{erf}(\alpha)\}, \tag{35}$$

where

$$\alpha = M^{\frac{1}{2}}(|y|-a)\{4|x|a\}^{-\frac{1}{2}}. \tag{36}$$

The centre of the wake is only known to within $O\{aM^{-\frac{2}{3}}\}$. Since the boundary layer has a thickness of order $aM^{-\frac{2}{3}}$ at its breakdown point (see figure 6), the wake emanates from a point where $|x| \sim aM^{-\frac{1}{2}}$. The theory requires that the maximum

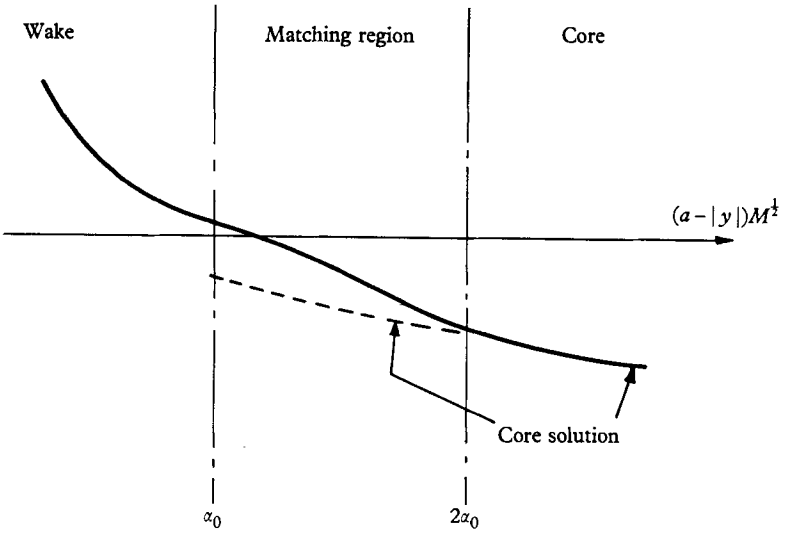

FIGURE 7. The profile of m in the matching region.

extent of the wake is small compared to a, i.e. we must have $M^{\frac{1}{2}} \gg 1$. Lastly, the boundary-layer theory is still valid where the wake meets the outer cylinder since $(\partial/\partial\xi)_{\text{wake}} \gg (\partial/\partial\zeta)_{\text{b. layer}}$.

Let us now examine how the wake and inner core solutions merge. Equation (29) shows that the inner core expansion is mathematically valid for $-\alpha \gg 1$, i.e. at the lower edge of the wake. At any given value of $(a-|y|)$ the order of magnitude of $(\partial m/\partial y)$, according to the wake and core solutions, will differ. However, where

$$(a-|y|) = a\alpha_0(x)M^{-\frac{1}{2}}, \tag{37}$$

they are of the same order of magnitude, α_0 being defined by

$$\exp\{\alpha_0^2\} = |Mx/a|^{\frac{1}{4}}\alpha_0^{\frac{1}{2}}. \tag{38}$$

At $\alpha = \alpha_0$, $|m_{\text{wake}}| \ll |m_L|$. Furthermore, for $\alpha \sim \alpha_0$, $-m_L$ is of order

$$(\partial m_L/\partial y)a\alpha_0 M^{-\frac{1}{2}}.$$

This suggests that the wake solution and the core expansion match up over a

region with width of order $a\alpha_0 M^{-\frac{1}{2}}$ (see figures 6, 7). For most of the wake $|x| \sim a$, and

$$\alpha_0 = \alpha_1 \text{ (say)} = \tfrac{1}{2}(\log M)^{\frac{1}{2}} + O\{[\log(\log M)]/[(\log M)^{\frac{1}{2}}]\}. \tag{39}$$

Equations (37) and (38) give the upper boundary of the matching region. This meets the inner cylinder where

$$(a - |y|) \sim a\alpha_2 M^{-\frac{2}{3}} \quad \text{(see figure 6)}, \tag{40}$$

with

$$\alpha_2 = 3^{-\frac{2}{3}}(\log M)^{\frac{2}{3}} + O\{\log(\log M)/(\log M)^{\frac{1}{3}}\}. \tag{41}$$

We will take equations (40) and (41) as defining the left-hand edge of the obscure region on the inner cylinder (see figure 6).

In §4(v) an estimate of the flow rate is derived. An error will arise since we can estimate m only in the left-hand (inner core) matching regions and n only in the right-hand ones. This error is of order $qa^3(\log M)^{\frac{2}{3}} M^{-\frac{1}{4}}$. The flow rate through the two obscure regions on the inner cylinder is of smaller magnitude. There will, of course, be a matching region at the outer edge of the wake. However, it may be verified without difficulty that the error term associated with this region is of smaller magnitude than that given above.

Now n does not change across the left-hand wakes. Thus

$$\left.\begin{aligned} V_z &= \tfrac{1}{4}q(b^2 - a^2)^{\frac{1}{2}}\{3 + \operatorname{erf}(\alpha)\}, \\ B_z &= -\mu P x B_0 - 2^{-1}(b^2 - a^2)^{\frac{1}{2}}\mu P B_0\{1 - \operatorname{erf}(\alpha)\}; \end{aligned}\right\} \tag{42}$$

in the right-hand wakes

$$\left.\begin{aligned} V_z &= \tfrac{1}{4}q(b^2 - a^2)^{\frac{1}{2}}\{3 + \operatorname{erf}(\alpha)\}, \\ B_z &= -\mu P x B_0 + 2^{-1}(b^2 - a^2)^{\frac{1}{2}}\mu P B_0\{1 - \operatorname{erf}(\alpha)\}. \end{aligned}\right\} \tag{43}$$

A qualitative picture of the current lines is given in figure 8. The velocity distribution (figure 9) is quite novel. The velocity drops by 50 % across the wake. This is because the boundary-layer current is split between the two cylinders for $|y| < a$.

(v) *The flow rate*

We can now estimate the flow rate Q. The dominant contribution Q_A comes from the core regions. The contribution from the wakes vanishes from symmetry considerations. The first non-vanishing correction comes from the matching regions, joining the wakes and the inner cores. Hence,

$$Q = Q_A\{1 + O(\{\log M\}^{\frac{3}{4}} M^{-\frac{3}{4}})\}, \tag{44}$$

where

$$\begin{aligned} Q_A &= 4\rho q \int_a^b (b^2 - y^2)\,dy + 2\rho q \int_0^a \{(b^2 - y^2)^{\frac{1}{2}} - (a^2 - y^2)^{\frac{1}{2}}\}^2 dy \\ &= (Pb^4/\nu M)(8\delta/3)\{1 + 4^{-1}(1 - \delta^2)(2K(\delta) - 3\delta) - 2^{-1}(1 + \delta^2)E(\delta)\}, \end{aligned} \tag{45}$$

where $\delta = (a/b)$. K and E are complete elliptic integrals of the first and second kind, respectively. $(\nu Q_A/Pb^4)M$ is plotted against (a/b) in figure 10. The flow rate, Q_0, for the case $B = 0$ (see, for example, Lamb 1945) is also plotted for comparison. Shercliff (1962) considered the expansion for the case of no inner cylinder.

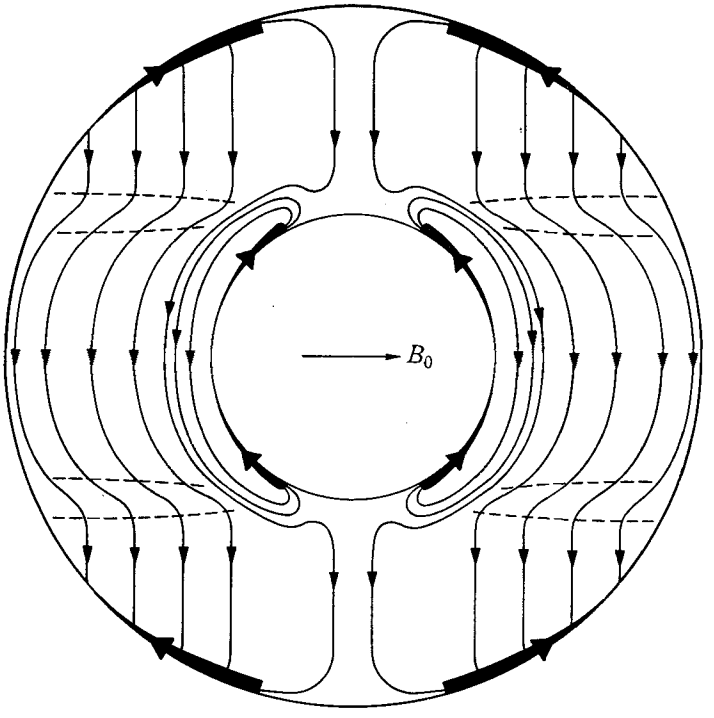

FIGURE 8. A qualitative picture of the current flow (the dashed lines denote the boundaries of the wakes).

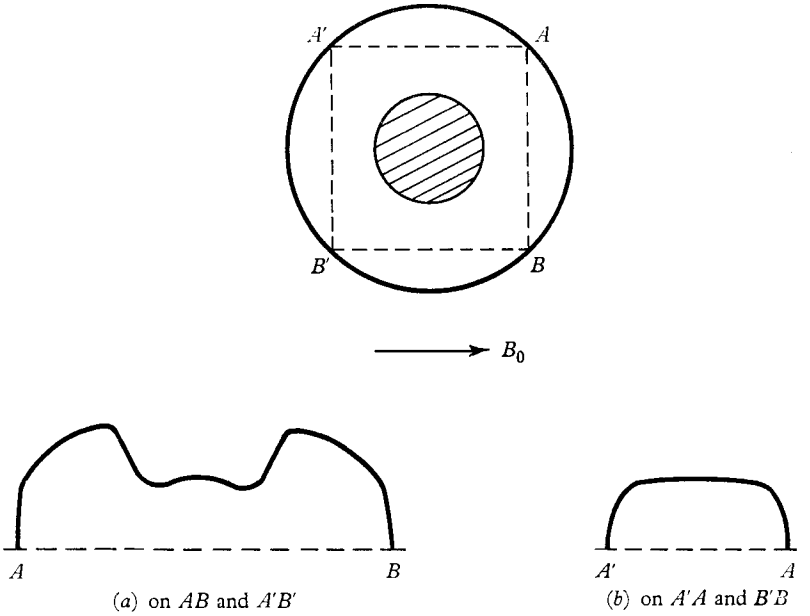

FIGURE 9. Some velocity profiles at high Hartmann numbers.

Because of the relatively small contribution from the obscure regions on the outer cylinder, Shercliff was able to obtain a correction term of order QM^{-1}. This is not possible in the present problem.

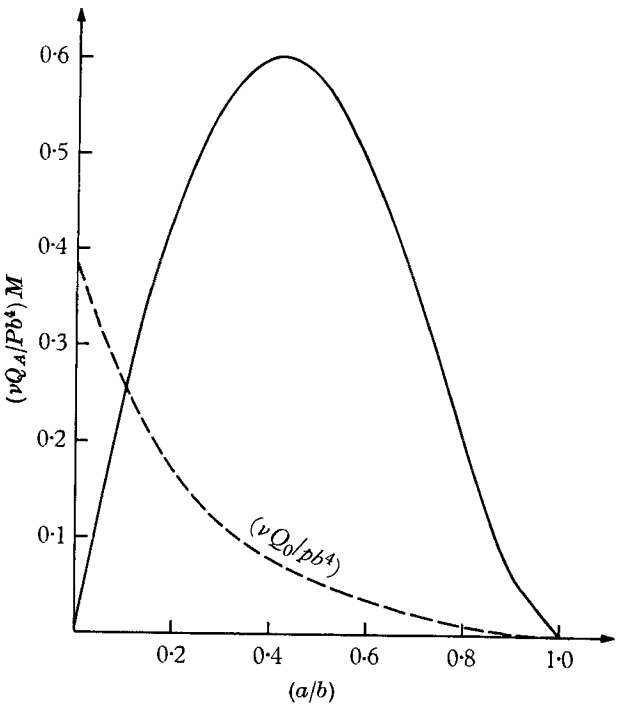

FIGURE 10. The flow rate at high Hartmann numbers (the flow rate, Q_0, for the case $B = 0$, is plotted for comparison).

5. High Hartmann number flow between eccentric cylinders of circular cross-section

Consider now the case of two eccentric circular cylinders (figure 11), the outer one being situated at $r = b$. The inner cylinder has radius a and is centred at (γ, ϵ), where $\{b - a \pm (\gamma^2 + \epsilon^2)^{\frac{1}{2}}\} \sim a$. The other remarks made at the beginning of §4, apply here also. Our main purpose in this section is to demonstrate that, for $\gamma \neq 0$, there is a net flow of current around the annulus. For this purpose, we need only consider the *zero order* solution (corresponding to $M = \infty$) in the various regions. The (zero order) solution, for the case $\gamma = 0$, is denoted by the superscript '0', e.g. m_r^0. The (constant) value of B_z at the inner cylinder C is as yet unknown. It will be found by applying the condition (10) at a later stage.

The outer core solution is

$$m_0 = m_0^0, \quad n_0 = n_0^0 \quad \text{and} \quad \mathbf{E} = \mathbf{E}^0. \tag{46}$$

In the right inner core

$$\left.\begin{aligned} m_R &= m_R^0, \quad n_R = n_R^0 - (q\gamma + sC), \\ \mathbf{E} &= \mathbf{E}^0 + \tfrac{1}{2}(sC + q\gamma)B_0\hat{\mathbf{y}}, \end{aligned}\right\} \tag{47}$$

and in the left inner core,

$$\left.\begin{aligned} m_L &= m_L^0 + (q\gamma + sC) \quad (n_L = n_L^0), \\ \mathbf{E} &= \mathbf{E}^0 - \tfrac{1}{2}(sC + q\gamma) B_0 \hat{\mathbf{y}}. \end{aligned}\right\} \tag{48}$$

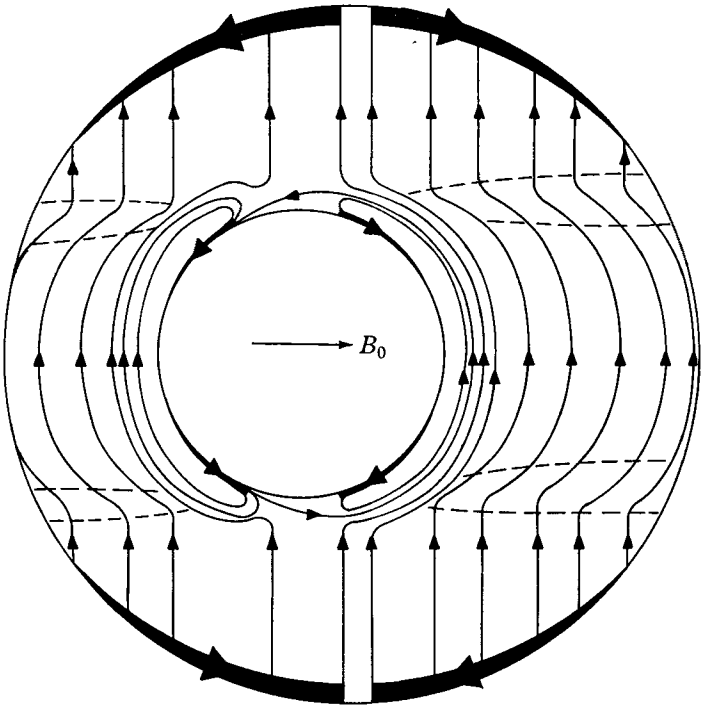

FIGURE 11. A qualitative picture of the current flow (eccentric cylinders).

Let us now apply condition (10), i.e. $\oint_L \mathbf{E}.\mathbf{dl} = 0$, where L is any closed contour lying within the outer cylinder and enclosing the inner one. It is convenient to take L as some rectangle whose sides are parallel to (Ox, Oy) and whose sides lie entirely in the core regions (except where two of them pass perpendicularly through the wakes). Now, considering only core contributions,

$$O = \oint_L \mathbf{E}.\mathbf{dl} = \oint_L \mathbf{E}^0.\mathbf{dl} + 2\int_{-a}^{a} B_0(sC + q\gamma)\,dy.$$

As shown in § 2,

$$\oint_L \mathbf{E}^0.\mathbf{dl} = 0.$$

Thus

$$C = -q\gamma s^{-1} = -\mu P B_0^{-1}\gamma. \tag{49}$$

The next order correction to (49) would normally come from considering the part of the path which lies in the wakes. In fact this contribution is identically zero, just as the 'wake term' in equation (44) is zero.

The value of C found above means that, to lowest order the core solutions (equations (46), (47) and (48)) are unaffected by the sideways displacement γ. Thus the flow rate, to the order found in § 4 (v), is unchanged from the case $\gamma = 0$. However, there is a qualitative change in the current distribution (see figure 11). This fact is easy to explain. As Shercliff (1956) has pointed out, the core velocity is proportional to the boundary-layer current. Thus these currents must be the same as for the case $\gamma = 0$. The *excess* current flowing up through the wider side of the core is $(P\gamma/B_0)$. This splits equally between the boundary layers on the opposite walls as indicated in figure 11, thereby offsetting the current deficit on that side. The wake solutions are the same as in the case $\gamma = 0$.

Clearly, the above analysis may be extended in a straightforward manner to the case of two (or more) cylinders of arbitrary cross-sections.

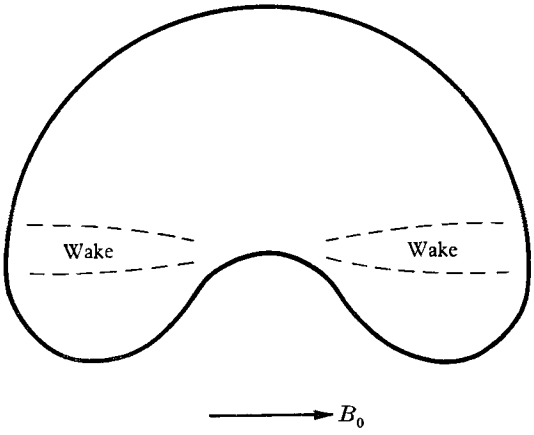

FIGURE 12. Another interesting cross-section for large Hartmann number flow.

6. Remarks

It would be of considerable interest to investigate the onset of turbulence in these flows, especially in view of the very novel velocity profiles (figure 9). The type of core division found in this paper will also occur for flow through a single cylinder with cross-section like that shown in figure 12. In the case of concentric cylinders, no wakes are present if the inner cylinder moves longitudinally with velocity $q(b^2-a^2)^{\frac{1}{2}}2^{-1}\hat{z}$. Similarly, with cylinders of any cross-section the wakes can be eliminated by moving the inner cylinders with appropriate velocities.

The constructive comments of the referees and of Dr H. K. Moffatt are gratefully acknowledged.

REFERENCES

GOLD, R. 1962 *J. Fluid Mech.* **13**, 505.
HASIMOTO, H. 1960 *J. Fluid Mech.* **8**, 61.
LAMB, H. 1945 *Hydrodynamics*, p. 586. Dover Press.
SHERCLIFF, J. A. 1953 *J. Fluid Mech.* **49**, 136.
SHERCLIFF, J. A. 1956 *J. Fluid Mech.* **1**, 644.
SHERCLIFF, J. A. 1962 *J. Fluid Mech.* **13**, 513.
UFLYAND, Y. S. 1961 *Sov. Phys. Tech. Phys.* **5**, 1194.